International Journal on Future Revolution in Computer Science & Communication Engineering
Volume: 4 Issue: 3
ISSN: 2454-4248
185 – 189

Automatic Liver Disease Diagnosis through B-mode Ultrasound Image

Karan Aggarwal,
ECE Deptt, M.M.E.C.
Mullana,
karan.170987@gmail.com,

Hardeep Singh Ryait,
ECE Deptt, BBSBEC
Fatehgarh Sahib,
hardeepsryait@gmail.com,

Manjit Singh Bhamrah
ECE Deptt, UCOE
Punjabi University,Patiala
manjitsingh_manjit@rediffmail.com

***Abstract*---**Diagnostic ultrasound is a useful and noninvasive method in clinical medicine. Although due to its qualitative, subjective and experience-based nature, ultrasound image interpretation can be influenced by image conditions such as scanning frequency and machine settings. In this paper, we present an automatic liver cirrhosis diagnosis system using ultrasound image matching. Given an input image, a preprocessing module is first performed to filter speckle noise and detect the extremely stable edge pattern which is defined by a similarity function using Hough transform. Furthermore, a template database is constructed to facilitate the detection of region of interests and liver cirrhosis classification. Then, support vector machine are employed to test a group of 30 in-vivo liver cirrhosis images from 18 patients, as well as other 30 liver images from 18 normal human volunteers. The results showed that the support vector machine was 92.4% in sensitivity for liver cirrhosis (LC) while neural network provided 89.31 % in LC [19], and the system was considered to be helpful for clinical and educational use.

***Keywords*---** *Cirrhosis liver, Texture, Hough Transform, Co-occurrences matrix, Support vector machine.*

*****

I. INTRODUCTION

Cirrhosis is a complication of many liver diseases that is characterized by abnormal structure and function of the liver. The diseases that lead to cirrhosis do so because they injure and kill liver cells and the inflammation and repair that is associated with the dying liver cells causes scar tissue to form. The liver cells that do not die multiply in an attempt to replace the cells that have died. This results in clusters of newly-formed liver cells (regenerative nodules) within the scar tissue.

Cirrhosis is considered to be the end stage of chronic hepatopathies which often leads to hepatocellular carcinoma. The diagnosis of the disease is best achieved by looking at the granular structure of the liver parenchyma and the aspects of the liver surface such as its unevenness and its contour as shown in Figure1.

The discrimination of cirrhosis from its preceding stages of fibrosis is based on visual aspect of the degree of nodularity present in the heterogeneous echo texture, which is often difficult to access visually [1]. Liver biopsy suffers from several important drawbacks like morbidity, observer variability and sampling variation [2] hence the interest in developing a noninvasive cirrhosis detection system. In literature there are a number of papers that propose the texture analysis methods applied on B-mode ultrasound images [3].

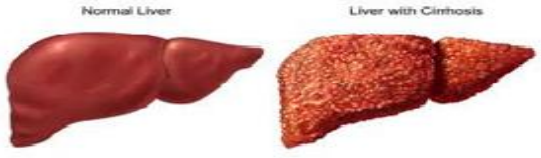

Figure 1: Represents granular structure of normal and cirrhosis liver

For quantitative image analysis many feature parameters have been proposed and used in developing automatic diagnosis system [5][6][7]. The several quantitative features are being used in diagnosis by ultrasonography. K. Ogawa [8][10] developed a classification method which used an artificial neural network to diagnose diffuse liver diseases. Another work [9]-[16] presents the classifier for diagnosis of normal liver (NL), chronic active hepatitis (CAH) and cirrhosis (CRH) more accurately. It has the potential to significantly assist radiologists to use this system for second opinion. The grey scale ultrasound images provide significant contribution to the diagnosis of liver diseases, however at the resolution it is difficult to diagnose active hepatitis and cirrhosis from normal liver [13][14]. A pattern recognition system can be considered in two stages, the first stage is feature extraction and the second is classification [15].

In this paper, we present an automatic liver cirrhosis diagnosis system using adaptive ultrasound image matching and a method is proposed to extract the liver features using the entropies of texture edge co-occurrence matrix based on ultrasound images, which is not sensitive to changes in emission frequency and gain. We construct a patient database in which each patient is associated with an ultrasound image and clinical information. For each database image, we compute its difference to the query image following the steps: ROI detection, extracting features from ROI and classification. Then, support vector machine are employed to test a group of 30 in-vivo liver cirrhosis images from 18 patients, as well as other 30 liver images from 18 normal human volunteers.

II. METHODOLOGY ADOPTED

There are a group of 30 in-vivo liver cirrhosis images from 18 patients, as well as other 30 liver images from 18 normal human volunteers. By using these images, five parameters have been detected and classify those images through SVM using MATLAB through block diagram as shown in Figure 2.

 ISSN: 2454-4248
185 – 189

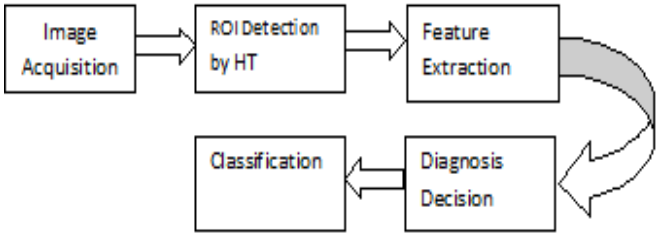

Figure 2 represent the steps involved to diagnose the liver

The Hough Transform (HT) represents an object with an R-table, which establishes the relationships between every edge point of the object and an object reference point. A visual object consisting of a number of edge points may undergo a geometric transformation with respect to a target image. Assume that there exists a subset of edge points that share the same geometric transformation mapping the visual object into the target image. The visual object can be described by the geometric relationship between the object centroid X^c and the centers of the regions in the object. Given an edge location X, the coordinates of X and X^c have the following relationship

$$\begin{bmatrix} x^c \\ y^c \end{bmatrix} = \begin{bmatrix} x+r\cos\alpha \\ y+r\sin\alpha \end{bmatrix} \quad (1)$$

where r denotes the Euclidean distance between X and X^c ,and α is the angle between the line passing X and X^c, and the x-axis. Note that, if the value of α is determined, the coordinates of X^R can be determined from those of X using Eq. (1). Accordingly, the R-table of the HT for representing a visual object can be constructed as

$$\begin{aligned} f_1 \quad & (r_1^1,\alpha_1^1)(r_1^2,\alpha_1^2),\ldots\ldots,(r_1^{n_1},\alpha_1^{n_1}) \\ f_2 \quad & (r_2^1,\alpha_2^1)(r_2^2,\alpha_2^2),\ldots\ldots,(r_2^{n_2},\alpha_2^2) \\ & \vdots \\ f_k \quad & (r_k^1,\alpha_k^1)(r_k^2,\alpha_k^2),\ldots\ldots,(r_k^{n_k},\alpha_k^{n_k}) \end{aligned} \quad (2)$$

Where $f_i, i = 1 \ldots\ldots k$, denote features for indexing these edges.

The edge points in a traditional R-table are indexed by the tangent slopes of the edge points, whereas the edges in the proposed R-table are indexed by the features of the edges. Unlike the exact matching of the original R-table indexing mechanism, a feature similarity between two features is calculated for indexing the proposed R-table.

Based on the user selected object template, we can detect the edge points of the template object, construct an R-table for these edge points, and perform the object search from the target image using the HT with the constructed R-table. Considering an edge point of feature *f*, which is a part of the target object in the target image, the centroid candidates (x^c, y^c) of the target object in the target image can be located on

$$\begin{bmatrix} x^c \\ y^c \end{bmatrix} = \begin{bmatrix} x_R + r(f)\,s\cos(\alpha(f)+\tau) \\ y_R + r(f)\,s\sin(\alpha(f)+\tau) \end{bmatrix} \quad (3)$$

where (x_R, y_R) are the coordinates of the center of *R*; *r(f)* and α (*f*) return the *r* and α values corresponding to the entry of the R-table of feature *f*; *s* and τ are the given scaling factor and rotation angle, respectively. Then, votes are cast for the parameter vectors (*s*,*τ*,x^c and y^c) in an s- *τ* -*x*-*y* parameter space. In practice, all possible values of s and τ should be evaluated; however, the parameters *s* and τ can be roughly equal to 1 and 0 in the training phase, respectively. Furthermore, a similarity measure (support) between an edge *e* of the target image and an edge *e'* of the template object is also calculated:

$$h(e,e') = \frac{2}{1+\varepsilon x p^{\rho \times \varepsilon(e,e')}} \quad (4)$$

where parameter ρ controls the speed at which the support *h* achieves one of its two extremes (0 and 1) according to the value of ε (*e*,*e*') , which is computed from the feature difference between *e* and *e'*. When the support value of an edge of the target image with respect to an edge of the template object is too low, that region is not considered to have a vote. This can dramatically reduce the number of spurious peaks in the resulting parameter space.

Parameters are:

A. Energy

$$ene = \sum_{i=0}^{N_g=1} \sum_{j=0}^{N_g-1} g^2(i,j)$$

This parameter is also called Angular Second moment [18] and Uniformity in [17], [19], [20].

Energy measures textural uniformity, i.e., pixel pairs repetitions; when the image patch under consideration is homogeneous (only similar gray level pixels are present) or when it is texturally uniform (the vector displacement always falls on the same (2, j) gray level pair, a few (possibly only one) elements of gray level co-occurrence matrix (GLCM) will be greater than 0 and close to 1, while many elements will be close to 0. In this case energy reaches values close to its maximum, equal to 1. Thus, high energy values occur when the gray level distribution over the window has either a constant or a periodic form [20]. This result means that energy is strongly uncorrelated to first order statistical variables such as contrast and variance. Indeed, energy may reach its maximum either with maximum or no variance and contrast values.

 ISSN: 2454-4248
185 – 189

B. Entropy

$$ent = -\sum_{i=0}^{N_g-1}\sum_{j=0}^{N_g-1} g(i,j).log\big(g(i,j)\big)$$

This parameter measures the disorder of an image. When the image is not texturally uniform, many GLCM elements have a very small value, which implies that entropy is very large. As an example, consider a window with completely random values of gray level pixel values (white noise).

C. Contrast

$$con = \sum_{i=0}^{N_g-1}\sum_{j=0}^{N_g-1} (i-j)^2.g(i,j) = \overline{\Delta_{con}}$$

Where

$$\Delta_{con} = (i-j)^2$$

Spatial frequency is the difference between the highest and the lowest values of a contiguous set of pixels. This definition holds for the GLCM contrast expression as well, in particular when the module of the displacement vector is equal to one. The conclusion is that the GLCM contrast tends to be highly correlated with spatial frequencies while the module of the displacement vector tends to one. With regard to the GLCM variance and contrast pair, the only condition that relates these two parameters to each other is the following: a sufficient, but not necessary, condition to keep contrast low is to maintain variance low (while the vice versa is not true). This result means that high contrast values imply high contrast texture, Le., first-order statistics contrast and GLCM contrast are strongly related. GLCM contrast and variance were also found to be highly correlated with the first order statistic standard deviation [21], but this condition, according to the theoretical discussion presented above, must be considered as a particular case for the contrast parameter.

D. Variance

$$var = \sum_{i=0}^{N_g-1}\sum_{j=0}^{N_g-1} (i-\mu)^2.g(i,j) = \overline{\Delta_{var}}$$

Where

$$\Delta_{var} = (i-\mu)^2$$

GLCM variance is a measure of heterogeneity and is strongly correlated to first order statistical variables such as standard deviation [21]. In particular, when a square image area is under textural investigation, the first order statistical variance is equal to the GLCM variance if the GLCM vector displacement is equal to 1 and if its investigation angle is equal to 0" or 90". Variance increases when the gray level values differ from their mean. Variance is not dependent on the GLCM parameter contrast, in particular when the module of the displacement vector tends to one, since a region may have low spatial frequencies and a low contrast value while its variance may have either a high or a low value (see the theoretical description of the GLCM contrast). Besides, variance requires more computation time than contrast.

E. Correlation

$$cor = \sum_{i=0}^{N_g-1}\sum_{j=0}^{N_g-1} (i-\mu).(j-\mu).g(i,j)\Big/_{\sigma^2} = \frac{\overline{\Delta_{cor}}}{\sigma^2}$$

Where

$$\Delta_{cor} = (i-\mu).(j-\mu).$$

GLCM correlation is expressed by the correlation coefficient between two random variables i and j , where i represents the possible outcomes in gray tone measurement for the first element of the displacement vector, while similarly j is associated with gray tones of the second element of the displacement vector. Correlation is a measure of gray tone linear-dependencies in the image [22], in particular, the direction under investigation is the same as vector displacement. High correlation values (close to 1) imply a linear relationship between the gray levels of pixel pairs.

As a limiting case of linear-dependency a completely homogeneous area may be considered, for which correlation is equal to 1.

III. SUPPORT VECTOR MACHINE

Pattern recognition by support vector machine (SVM) may be stated as follows (Burges, 1998): Given a training set (***xi***, *yi*) (where ***xi*** comprises the

input features, $yi \in \{\pm 1\}$ is the classification output, i=1, 2,… N, and N is the number of samples). Optimal margin classification of linearly separable patterns is achieved by finding a hyper plane to separate the two classes {+1, −1} on either side of the hyper plane. The decision surface (the hyper plane) is as follows:

$$f(x) = sgn\left(\sum_{i-1}^{N} y_i a_i (x_i.x) + b\right)$$

where, the coefficients αi and b can be determined by solving the large-scale quadratic programming problem:

$$W(\alpha) = \sum_{i-1}^{N} \alpha_i - \frac{1}{2}\sum_{i,j-1}^{N} \alpha_i \alpha_j y_i y_j (x_i.x_j)$$

 ISSN: 2454-4248
185 – 189

which is subject to the constraints

$$\sum_{i-1}^{l} \alpha_i y_i = 0, 0 \leq \alpha_i \leq C \; for \; i - 1,2,\ldots.l$$

The parameter C corresponds to assigning a penalty to tune the tradeoff between minimizing empirical risk (e.g. training errors) and the complexity of the machine. Upon training, only a fraction of the αi terms are nonzero. For those αiS that are nonzero, the corresponding training examples must be nearest to the margins of the decision boundary. These examples are called support vectors.

In most problems, the data are not linearly separable. In order to apply nonlinear transforms to the original data, multiplying all the terms in the feature vector with each other can create a higher dimensional vector. The basic idea is to map the data into another feature space F where the patterns are linearly separable with a high probability via a nonlinear map $\Phi: R^m \rightarrow F$ and implement the above linear algorithm in F. So, the solution has the form:

$$f(x) = \text{sgn}\left(\sum_{i-1}^{N} y_i \alpha_i \Phi(x_i)\Phi(x) + b\right)$$

Accordingly, F usually must have very high dimensionality in order to be linearly separable. This can be resolved based on two observations: First, although some mappings have very high dimensionalities, their inner products can be easily computed and second, all the Φ mappings used in the SVM occur in the form of an inner product. So, all the occurrences of inner product resulting from two mappings can be replaced with the kernel function K defined as:

$$K(x, y) = \Phi(x) \cdot \Phi(y)$$

Then, without considering the mapping Φ explicitly, a nonlinear SVM can be constructed by selecting the proper kernel, and the decision function becomes:

$$f(x) = \text{sgn}\left(\sum_{i-1}^{N} y_i \alpha_i K(x_i, x) + b\right)$$

Polynomial kernel function as one of the three common type kernel functions of SVM is used as:

$$K(x_i, x) = \left(\gamma x_i^T . x + c\right)^d, \gamma > 0$$

In this study, γ=1, c=1, and d=3.

IV. RESULTS AND DISCUSSION

The performance of the proposed system is evaluated with various test images, where each of them is labeled by radiologist that is liver cirrhosis. The patient database with 40 test samples is separated into two parts: the training database and the test database. These ultrasound images with 430x380 pixels and 256 grays were obtained from B-mode ultrasound imaging system with different tissue harmonic 5.0 and 16 fps.

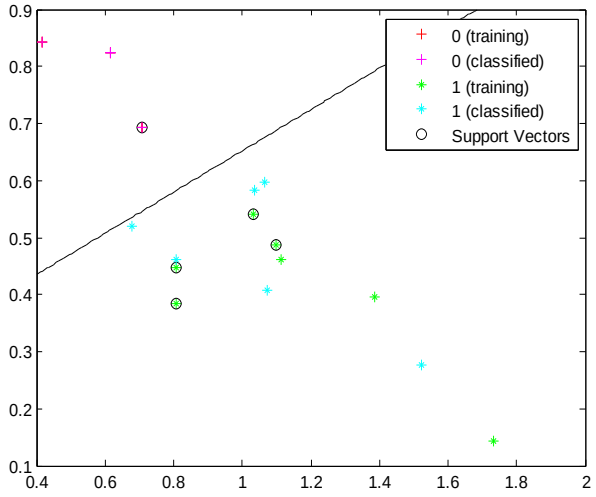

Figure 3 Graph between contrast and correlation of cirrhosis & normal liver

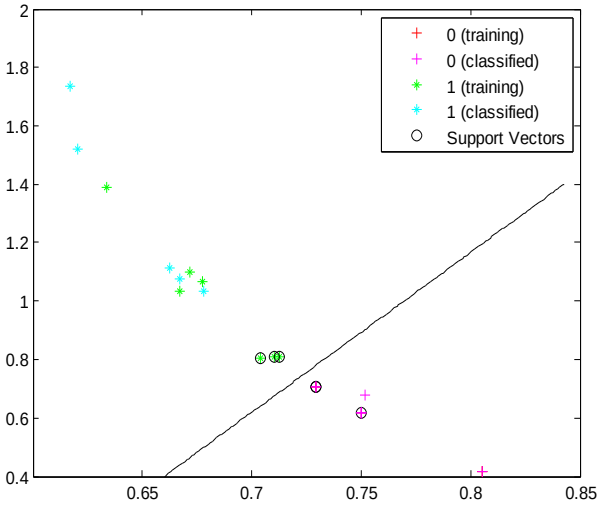

Figure 4 Graph between energy and contrast of cirrhosis and normal liver

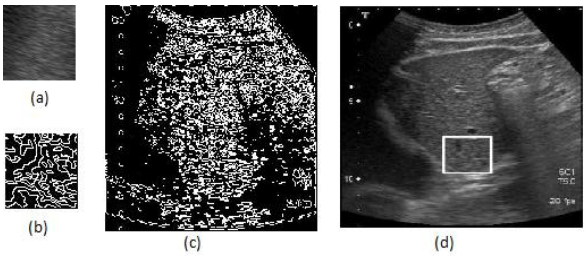

Figure 5 The automatic ROI selection using HT: (a) the original template image, (b) the edge pattern of (a), edge pattern of the query image, (d) the detected ROI in the query image.

Figure 5 shows an example to selection of the ROI from a query image. The selected ROI is much similar with the template in terms of feature difference.

For a fair comparison, we test the performance for both methods under the same condition --the ROI is selected manually to answer a query image.

 ISSN: 2454-4248
185 – 189

TABLE 1shows classification accuracy

Classifier	Classification Accuracy
Neural Network Classifier	89.31%
SVM Classifier	92.4%

Table 1 shows the classification accuracy for both methods including neural network and support vector machine for cirrhosis liver detection. In practice, we fix the ROI to the central area of the input query image for classification.

Experimental results show that the proposed method outperforms on last methods (neural network) in diagnosis normal and cirrhosis liver system based on ultrasound images.

V. CONCLUSION

In this paper, we have presented the method to construct an automatic system for liver disease prediction. The contributions of the paper include: (1) a training procedure is proposed to enhance the quality of clinical ultrasound images and to obtain the stable parameter for detecting the maximally stable edge pattern; (2) an automatic ROI detection is presented using HT; (3) an adaptive image matching approach is presented to predict the possibility of liver cirrhosis for a patient based on the patient database and the input ultrasound image. Then we proposed an image classification method with texture features based on SVM. The results showed that the support vector machine was 92.4% in sensitivity for liver cirrhosis (LC) while neural network provided 89.31 % in LC. From the experiments results on high- resolution arial images, it has been shown that this method can achieve better results than traditional pixel-based classification method with spectral information used only. The experiment results show that this method is feasible and it can exert the virtues of both spectral and texture features.

REFERENCES

[1]. Jitendra Vermani, Vinod Kumar. Naveen Kalra and Noranjan Khandelwal,"Prediction of Cirrhosis from Liver Ultrasound B-Mode Images based on Laws' Masks Analysis" pp.1-5 ,2011

[2]. P. Bedossa, D. Dargere, and V. Paradis, "Sampling variability of liver fibrosis in chronic hepatitis C," Hepatology, vol. 38, pp. 1449-1457, 2003.

[3]. S. Nedevschi, C. Vicas, M. Lupsor, R. Badea, and M.Grigorescu, "The employment of textural and non textural image analysis algorithms in assessing the diffuse liver diseases," Automat. Comput, Appl. Math. , vol. 17, pp. 12-17, 2008.

[4]. C. Vicas, S. Nedevschi, M. Lupsor, and R. Badea, "Fibrosis detection from ultrasound imaging. The influence of necro-inflammatory activity and steatosis over the detection rates," Automat. Comput, Appl. Math.,vol. 16, .pp. 26-32, 2007

[5]. Abou zaid Sayed Abou zaid and Mohamed Waleed Fakhr, "Automatic Diagnosis of Liver Diseases from Ultrasound Images", IEEE Transactions on Medical Imaging (2006) 313-319.

[6]. Y-N Sun and M-H Horng, Ultrasonic image analysis for Liver Diagnosis,Proceeding of IEEE Engineering in Medicine and Biology (Nov 1996) 93-101

[7]. A.Takaishi, K. Ogawa, and N. &a, "Pattern recognition of diffuse liver diseases by neural networks in ultrasonography," in Proc. of the IEICE (The Institute of Electronics, Information and Communication Engineers) Spring conference 1992 (March), p.6-202.

[8]. K. Ogawa and M. Fukushima, "Computer-aided Diagnostic System for Diffuse Liver Diseases with Ultrasonography by Neural Networks", IEEE Transactions on Nuclear Science vol.45-6, 1998 pp.3069-3074.

[9]. Y.M. Kadah, "Statistical and neural classifiers for ultrasound tissue characterization", in Proc. A NNIE-93, Artificial Neural Networks in Engineering, Roolla, MO, 1993.

[10]. K. Ogawa, N. Hisa, and A. Takaishi, "A study for quantitative evaluation of hepatic parenchymal diseases using neural networks in B-mode ultrasonography," Med Image Technolgy, vol.11, pp.72-79, 1993.

[11]. M. Fukushima and K. Ogawa, "Quantitative Tissue Characterization of Diffuse Liver Diseases from Ultrasound Images by Neural Network", IEEE Transactions on Medical Imaging, vo1. 5, pp.1233-123,1998.

[12]. R.M.Haralick, K. Shanmugam, J.Din, "Texture features for image classification", IEEE Transactions on System, Man and Cybernetics vol.SMC-3, pp. 610-62,1973.

[13]. Elif Derya Übeylı and İnan Güler, "Feature extraction from Doppler ultrasound signals for automated diagnostic systems", Computers in Biology and Medicine vol. 35, Issue 9, pp 735-764, November 2005.

[14]. Stavroula G. Mougiakakou and Ioannis K. Valavanis, "Differential diagnosis of CT focal liver lesions using texture features, feature selection and ensemble driven classifiers", Artificial Intelligence in Medicine vol. 41, Issue 1,pp. 25-37, September 2007.

[15]. Elif Derya Übeylı and İnan Güler, "Improving medical diagnostic accuracy of ultrasound Doppler signals by combining neural network models", Computers in Biology and Medicine vol. 35,pp 533-554, 2005.

[16]. Y.M. Kadah, A.A. Farag, M. Zurada, A. M. Badawi, and A.M. Youssef, "Classification algorithms for quantitative tissue characterization of diffuse liver diseases from ultrasound images:, IEEE Transactions on Medical Imaging vol. 15, no. 4,pp. 466-477, 1996.

[17]. D. G. Barber and E. F. LeDrew, "SAR sea Ice discrimination using texture statistics: A multivariate approach," Photogram Eng. Remote Sensing, vol. 57, no. 4, pp. 385-395, 1991.

[18]. P. Gong, J. D. Marceau, and P. J. Howarth, "A comparison of spatial feature extraction algorithms for land-use classification ith SPOT HRV data," Remote Sensing Environment., vol. 40, pp. 137-151, 1992.

[19]. Qiang LIU, Van-hong MA, Ning Wang, Yi-hui LIU,,Shao-qing Wang, Li-juan Wang, Jin-yong Cheng Jie Chen, Dong-yue Yu," 31P-MRS Data Analysis of Liver Based on Self-organizing Map Neural Networks", pp 151-153,2009.

[20]. M. E. Shokr, "Evaluation of second-order textural parameters for sea ice classification in radar images," J. Geophys. Res.. vol. 96, no. C6, pp. 10625-10640, 1991.

[21]. 0.Dikshit, "The classification of texture in remotely sensed environmental imagery," Ph.D. dissertation, Univ. Cambridge, Cambridge, UK, 1992.

[22]. R.Cossu, "Segmentation by means of textural analysis," Pixel, vol. I, no. 2, pp. 21-24, 1988.

[23]. T. K. Hirose, L. McNutt, and J. S. Paterson, "A study of textural and tonal information for classifying sea ice SAR imagery," Proc. IGARSS '89, Vancouver, Canada, pp. 747-750, 1989.